RP Current Trends In Applied Sciences
Vol. 2, No. 3 (July – September 2023) pp. 46–50
e-ISSN: 2583-7486

RESEARCH PLATEAU PUBLISHERS

Cite this article: I. Sk, N. Pakhira, Electronic properties of doped chalcopyrite semiconductors $CuBSe_{1-x}Te_x$ (x = 0.125, 0.25): a first principle study, *RP Cur. Tr. Appl. Sci.* **2** (2023) 46–50.

Original Research Article

Electronic properties of doped chalcopyrite semiconductors $CuBSe_{1-x}Te_x$ (x = 0.125, 0.25): a first principle study

Ismail Sk[1,*], Nandan Pakhira[2]
[1]Department of Physics, Bajkul Milani Mahavidyalaya, Purba Medinipur – 721655, West Bengal, India
[2]Department of Physics, Kazi Nazrul University, Asansol -713340, West Bengal, India
*Corresponding author, E-mail: ismailsk44@gmail.com

ARTICLE HISTORY
Received: 11 June 2023
Revised: 26 August 2023
Accepted: 27 August 2023
Published online: 16 Sept. 2023

KEYWORDS
Crystal structure;
Chalcopyrite; DFT

ABSTRACT
In the last few decades, chalocopyrite semiconductor compounds have received increased theoretically as well as experimental attention due to their potential technological applications. Here we report the electronic properties of, yet to be experimentally investigated, commensurately doped compounds $CuBSe_{1-x}Te_x$ (x = 0.125, 0.25) using first principle electronic structure methods based on density functional theory (DFT). These compounds can be prepared (computationally) by replacing one or two Se atom(s) by Te atom(s) in a given unit cell for 12.5% and 25% dopings, respectively. This new type of doped chalcopyrite semiconductors has crystal structures different from the parent compound $CuBSe_2$. The electronic structure of these doped compounds have been studied under generalized gradient approximation (GGA) using ultrasoft pseudo-potentials as implemented in open-source Quantum Espresso package. We also report the projected density of states and total density of states of these compounds. The analysis of the density of states shows that the conduction bands are mainly formed due to the contributions of the s, p orbital of B and Se atoms and with a smaller contribution from the p-Cu orbital and s, p states of Te atom. On the other hand, the valence bands are formed due to major contribution of p-(B, Se, and Te) states and a small contribution from the d-orbital of Cu atom with s-(B, Se, and Te) states. The estimated direct band gap energies are found to be 1.141 eV and 1.105 eV, respectively, which are less as compared to the parent $CuBSe_2$ (E_g = 1.473 eV) compound.

1. Introduction

During the past few decades, there has been a growing interest in ternary chalcopyrite compounds with formula $A^I B^{III} X_2^{VI}$ due to their significant potential in electro-optical and opto-electronic devices [1]. These metal-based chalcogenide materials also show promise for non-linear optical applications in the infrared region of the electromagnetic spectrum [2]. Ternary chalcogenide compounds, which consist of at least one electro-positive element and chalcogenide anion (a Group VI element), form a diverse group of semiconductors with varying structural, electrical, and optical properties. They have also shown potential in solar cell devices and thermoelectric applications [3-5]. In recent years, there has been considerable research focus on copper-based compounds [6] due to the remarkable progress in the efficiency of solar cells based on materials like copper indium sulphide, $CuInS_2$ (CIS) [7] and copper indium gallium selenide, $CuInGaSe_2$ (CIGS) [8-10]. Among the class of ABX_2compounds, which includes chalcogenides such as $CuBX_2$ (X = S, Se, Te), $CuBS_2$ and $CuBSe_2$have been extensively studied both theoretically and experimentally for their electronic and transport properties. These compounds have optimum electronic band gap energies of 3.61 eV and 3.13 eV, respectively [12, 13]. Their band gap energies, along with those of other compounds in this class, fall within the ultraviolet (UV) region, making them potential candidates for UV photo detectors, UV light emitters, and electronic power applications. In this study, we investigate a new class of doped chalcopyrite semiconductors, $CuBSe_{1-x}Te_x$, which have not yet been experimentally explored. We focus on two commensurate filling fractions, x = 0.125 and x = 0.25, using first-principle electronic structure methods [14-15] implemented in the open-source Quantum Espresso package [16]. The compounds involving boron elements play a crucial role in the electronic structure of the system as a sp-hybridized state [17]. The main objective and goal of this study is to understand role of chalcogen substitution in homogeneous chalcopyrite semiconductors. The doped semiconductors are expected to have different band gap than pure semiconductors. As a result these transparent p-type semiconductors can show transparency at different wave lengths than the parent compounds. Also the substitution doping can modify the nature of band gap from direct to indirect and vice versa. The dopant atom with different atomic radii and electronegtivity can cause structural distortion and chemical inhomogeneity. This in general can change the elastic and optical properties of a given semiconductor.

2. Materials and methods

In this article, we have initially started with the parent $CuBSe_2$ compound. The lattice information of $CuBSe_2$was obtained from the material project website [18]. The parent compound consists of four Cu atoms, four B atoms, and eight

Se atoms in a tetragonal cell with lattice parameters of a = 5.29 A°, and c = 9.67 A°, belonging to space group I-42d, as depicted in Figure 1 [18].

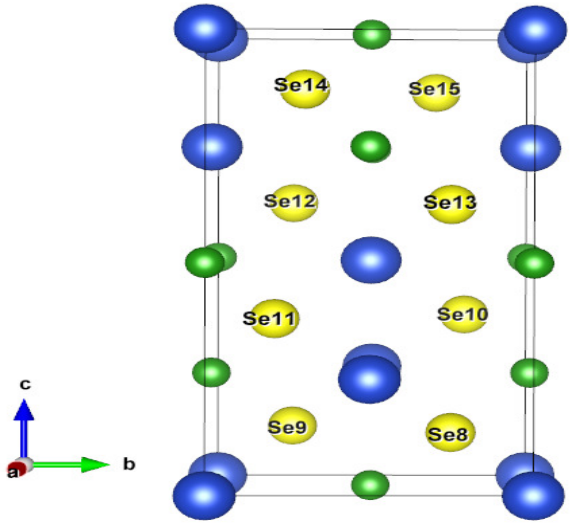

Figure 1: The crystal structure of$CuBSe_2$. Blue: Cu, Green: B, Yellow: Se.

To investigate the doping effects, we introduced one and two Te atoms into the parent$CuBSe_2$, compound, achieving commensurate filling in a given unit cell and effective doping concentrations of 12.5% and 25%, respectively. The VESTA software [19] was used for visualization, and the free software BURAI [20] was used for generating input files and visualization. We employed the Perdew-Burke-Ernzerhof (PBE) exchange correlation (XC) functional within the framework of generalized gradient approximation (GGA) [21]. To achieve good numerical accuracy, we set kinetic energy and charge density cutoffs to 25 Ry and 225 Ry, respectively. Subsequently, we relaxed the structure using Quantum Espresso and determined the structure parameters, possible structures, and electronic band gap energies for the two doped systems. For the relaxation and electronic band structure calculations, we employed a k-mesh grid of size 4×4×2, covering the entire Brillouin zone. Additionally, a 6×6×3 k-mesh was used for calculating the density of states. Throughout the calculations, an energy convergence criteria of 10^{-6} Ry was maintained for both systems. The band structures were plotted along a path involving high symmetry points.

3. Results and discussion

In this paper, we present the electronic band structure of $CuBSe_{1-x}Te_x$and the projected density of states (PDOS) to elucidate role of doping in chalcopyrites. First we analyze the electronic band structure and PDOS of the parent compound$CuBSe_2$.The band gap energy of the parent compound is determined to be 1.473 eV (experimental value. 1.49 eV [18]) and located at the Γ point as illustrated in Fig. 2 (a). The electronic band structure is further explained using PDOS, depicted in Fig. 2 (b) on the right side of the panel. The conduction band is primarily contributed by the p-states of B atom, with a minor contribution from the s- states of B atom as well as s, p- states of Se element. The valence bands in the energy range of -10 eV to 0 eV are predominantly formed by the d-orbital of the Cu element, with a slight contribution from the p-orbital of the B and Se atoms as well as the s-orbital of the B atom. Additionally, the peaks observed at -15 eV arise due to dominant contribution of the s-orbital of the Se atom and partial contribution of B atom. To investigate the effect of doping, we introduce a Te element with commensurate filling in a given unit cell at doping levels of 12.5% and 25%. The crystal structures of the $CuBSe_{1-x}Te_x$compound with 12.5% and 25% doping are shown in Fig. 3 (a, b). Subsequently, the structures are optimized, and the resulting band structures and density of states are analyzed. The calculated lattice parameters, possible band gap energies, and other relevant data are summarized in the table. Overall, our study provides valuable insights into the band structure and properties of the $CuBSe_{1-x}Te_x$compounds, shedding light on the impact of doping on their electronic structure and potential applications.

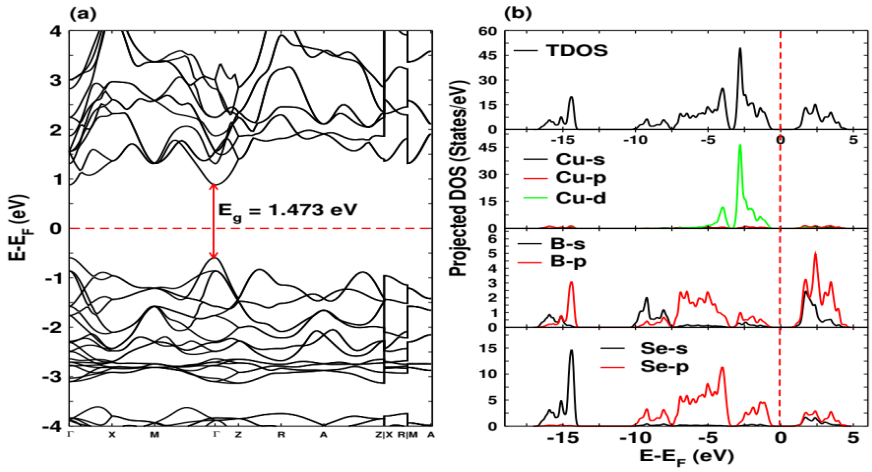

Figure 2: (a) The band structure and (b) the projected density of states of $CuBSe_2$ semiconductor The Fermi energy level isset to zero and assigned by red dashed line.

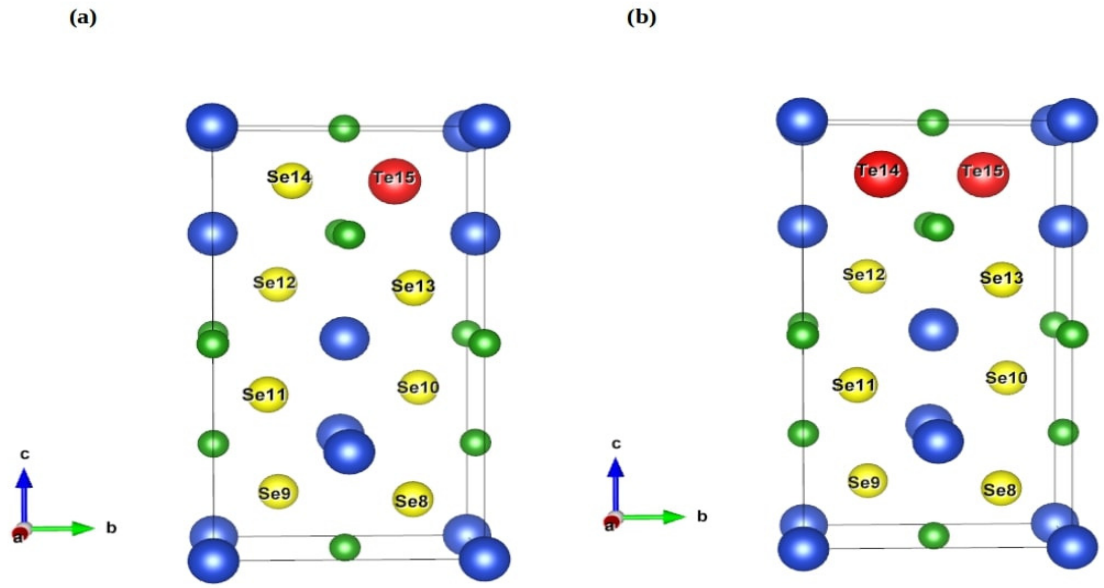

Figure 3: The crystal structure of $CuBSe_{1-x}Te_x$ with (a) 12.5 % (b) 25 % Te element doping. Blue: Cu, Green: B, Yellow: Se and Red: Te atom.

Table 1: Calculated lattice parameters and band gap energies

Systems	a (A°)	b (A°)	c (A°)	Structure	Band Gap (eV)
$CuBSe_2$	5.28575	5.28757	9.67274	Tetragonal	1.473
$CuBSe_{1-x}Te_x(x = 0.125)$	5.16990	5.13260	9.37180	Orthorhombic	1.141
$CuBSe_{1-x}Te_x(x = 0.25)$	5.21206	5.13342	9.43398	orthorhombic	1.105

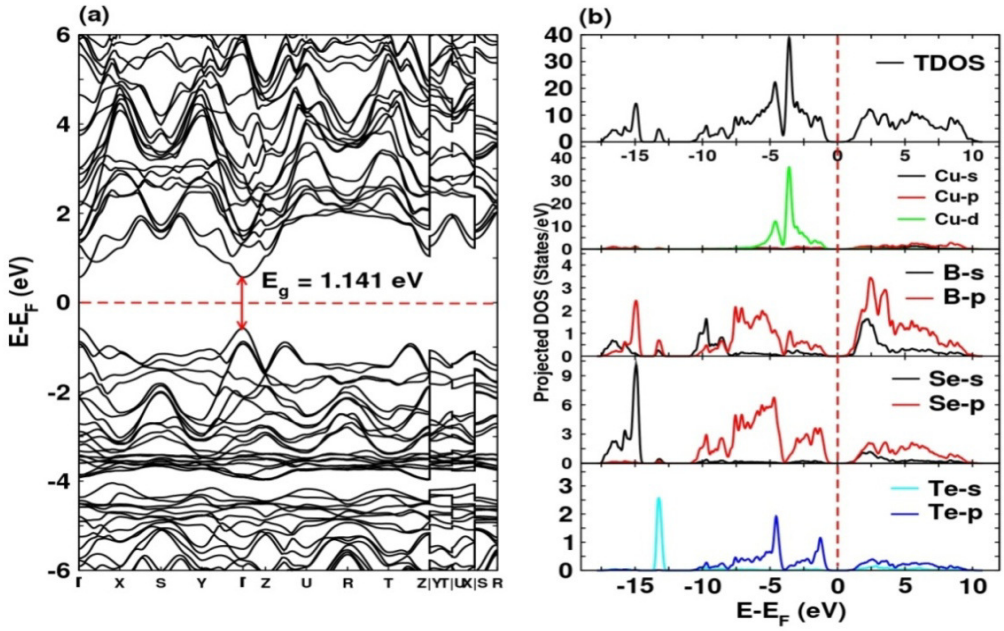

Figure 4: (a) The band structure and (b) the projected density of states of $CuBSe_{1-x}Te_x$ semiconductor with 12.5 % Te doping. The Fermi energy level is set to zero and assigned by red dashed line.

Figure 4 (a) and Figure 5 (a) illustrate the band structures of $CuBSe_{1-x}Te_x$ semiconductors with 12.5% and 25% Te doping, respectively. In both cases, the maximum valence band and the minimum conduction band are located at the Γ point. The calculated band gap energies are found to be 1.141 eV and 1.105 eV, respectively, indicating that these materials exhibit direct band gap characteristics. The decrease in band gap energy can be attributed to the increased substitution of Te atoms in place of Se atoms, resulting in a more distorted structure. This substitution leads to a decrease in the band gap compared to the parent compound. This effect is due to the additional major contribution of the electron density from the

p-orbital of the Te atom into the Fermi level. The introduction of Te atom(s) as impurities in the parent compound creates impurity levels near the valence band, as shown in Figure 4 and Figure 5. Additionally, the band structure of the 25% doping system exhibits less dispersion compared to the 12.5% doping case. To gain a comprehensive understanding of the atomic contributions to the electronic band structure, we calculate the projected density of states (PDOS) as depicted in Figure 4 (b) and Figure 5 (b). The red dashed line represents the Fermi level, which is set to zero. The analysis of the density of states curves reveals several categories, with bands formed both above and below the Fermi level. Overall, the PDOS analysis provides valuable insights into the individual atomic contributions and helps in comprehending the electronic band structure of the materials under investigation.

Above the Fermi level, the conduction bands primarily result from a significant contribution of p-(B, Se, Te) states, with smaller contributions from s-(B, Se, Te) and p-(Cu) states. Below the Fermi level, the valence bands can be categorized as follows: In the energy range of 0 eV to -7.5 eV, the valence bands are mainly formed by the dominant contribution of the d-orbital of the Cu atom, accompanied by a minor contribution from p-(B, Se, and Te) states. From -7.5 eV to -10.5 eV, the valence bands are primarily influenced by the substantial contribution of p-(B, Se, and Te) states, along with a small contribution from s-(B) states. In the energy range from -10.5 eV to -12.5 eV, there exists a significant gap that remains unaffected by the contribution of any specific atom's states. At around -13 eV, a small peak arises due to the major contribution of s-states from the Te element. In the energy range of -14.5 eV to -17.5 eV, the valence bands are characterized by a large contribution from p-(B) and s-(Se) states, accompanied by a small contribution from s-(B) states. The analysis of these energy windows provides insights into the contributions of various atomic states to the formation of valence bands below the Fermi level in the $CuBSe_{1-x}Te_x$ compounds.

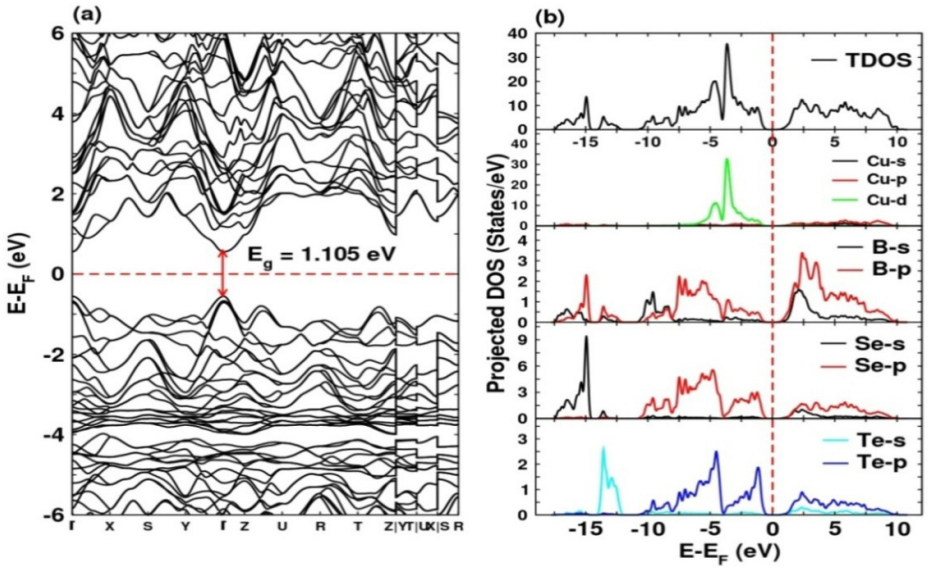

Figure 5: (a) The band structure and (b) the projected density of states of $CuBSe_{1-x}Te_x$semiconductor with 25 % Te doping. The Fermi energy level is set to zero and assigned by red dashed line.

4. Conclusions

The electronic properties of, yet to be experimentally investigated, $CuBSe_{1-x}Te_x$ (x = 0.125, 0.25) have been computationally studied in this work. Utilizing first-principle methods based on density functional theory (DFT) implemented in the open-source Quantum Espresso package, we have investigated the effects of doping a Te element into $CuBSe_2$compounds with commensurate filling fraction of 12.5% and 25%, respectively. Our investigation is focused on analyzing the band structure and density of states of doped $CuBSe_{1-x}Te_x$compounds. The calculated band gap energies were determined to be 1.141 eV and 1.105 eV for 12.5% and 25% dopings, respectively. These band gaps are lower compared to the parent $CuBSe_2$compound (E_g = 1.473 eV). Our study also indicates that these semiconductor systems exhibit direct band gaps. To provide a comprehensive explanation of the band structure in $CuBSe_{1-x}Te_x$chalcopyrite semiconductors, we utilized the projected density of states curves. The optical and mechanical properties of these doped systems will be further investigated in a future work. Overall, our computational study sheds light on the electronic properties of $CuBSe_{1-x}Te_x$compounds, highlighting their potential as direct band gap semiconductors. Further exploration of the optical and mechanical characteristics will enhance our understanding of these doped materials.

Acknowledgements

This work is partially supported by WB-DSTBT research grant no. STBT- 11012(26)/31/2019-ST SEC. One of us (NP) would like to acknowledge hospitality of IIT, Kharagpore. One of us (IS) would like to thank Bajkul Milani College authority for giving me an opportunity to pursue research as a Ph. D. scholar.

References

[1] S.N. Rashkeev, S. Limpijumnong, W.R.L. Lambrecht, Second-harmonic generation and birefringence of some ternary pnictide semiconductors, *Phys. Rev. B* **59** (1999) 2737.

[2] I. Chung, M.G. Kanatzidis, Metal chalcogenides: A rich source of nonlinear optical materials, *Chem. Mater*. **26** (2014) 849-869.
[3] S. Mishra, B. Ganguli, Effect of structural distortion and nature of bonding on the electronic properties of defect and Li-doped $CuInSe_2$ chalcopyrite semiconductors, *Solid State Commun*. **151** (2011) 523-528.
[4] S. Mishra, B. Ganguli, Effect of structural distortion and nature of bonding on the electronic properties of defect and Li-substituted $CuInSe_2$ chalcopyrite semiconductors, *J. Alloys Comp*. **512** (2012) 17-22.
[5] A. Reshak, Transport properties of mixed $CuAl(S_{1-x}Se_x)_2$ as promising thermoelectric crystalline materials, *J. Phys. Chem. Solids* **78** (2015) 46-52.
[6] P. Dey, J. Bible, S. Datta, S. Broderick, J. Jasinski, M. Sunkara, M. Menon, and K. Rajan, Informatics-aided bandgap engineering for solar materials, *Comp. Mater. Sci*. **83** (2014) 185-195.
[7] A. Tapley, D. Vaccarello, J. Hedges, F. Jia, D. Love, Z. Ding, Preparation and characterization of $CuInS_2$ nanocrystals for photovoltaic materials, *Phys. Chem. Chem. Phys*. **15** (2012) 1431-1436.
[8] I. Repins, M.A. Contreras, B. Egaas, C. DeHart, J. Scharf, C.L. Perkins, B. To, R. Noufi, 19·9%-efficient ZnO/CdS/$CuInGaSe_2$ solar cell with 81·2% fill factor, *Prog. Photovolt.: Res. Appl*. **16** (2008) 235-239.
[9] D.C. Perng, J.W. Chen, C.J. Wu, Formation of $CuInAlSe_2$ film with double graded bandgap using Mo(Al) back contact, *Solar Energy Mater. Solar Cells* **95** (2011) 257-260.
[10] P. Jackson, D. Hariskos, E. Lotter, S. Paetel, R. Wuerz, R. Menner, W. Wischmann, M. Powalla, New world record efficiency for Cu(In,Ga)Se_2 thin-film solar cells beyond 20%, *Prog. Photovolt.: Res. Appl*. **19** (2011) 894-897.
[11] V. Sousa, Chalcogenide materials and their application to non-volatile memories, *Microelectro. Eng*. **88** (2011) 807-813.
[12] T. Kajiki, Y. Hayashi, H. Takizawa, High-pressure synthesis of a new copper thioborate, $CuBS_2$, *Mater. Lett*. **61** (2007) 2382-2385.
[13] L.J. Chen, J.D. Liao, Y.J. Chuang, Retraction: Self-assembled chalcopyrite ternary semiconductor CuBSe2 nanocrystals: solvothermal synthesis and characterization, *Cryst. Eng. Comm*. **24** (2022) 3109.
[14] P. Hohenberg, W. Kohn, Inhomogeneous electron gas, *Phys. Rev*. *B* **136** (1964) 864.
[15] W. Kohn, L.J. Sham, Self-consistent equations including exchange and correlation effects, *Phys. Rev*. **140** (1965) A1133.
[16] Paolo Giannozzi et al., QUANTUM ESPRESSO: a modular and open-source software project for quantum simulations of materials. *J. Phys.: Condens. Matter* **21** (2009) 395502.
[17] I. Sk, N. Pakhira, Role of spin-orbit coupling effects in rare-earth metallic tetra-borides: a first principle study, *Eur. Phys. J. B* **96** (2023) 29.
[18] A. Jain, S.P. Ong, G. Hautier, The Materials Project: A materials genome approach to accelerating materials innovation, *APL Materials* **1** (2013) 011002.
[19] K. Momma, F. Izumi, VESTA 3 for Three-Dimensional Visualization of Crystal, Volumetric and Morphology Data, J. Appl. Cryst. **44** (2011) 1272-1276.
[20] Online article: https://nisihara.wixsite.com/burai/
[21] J.P. Perdew, K. Burke, M. Ernzerhof, Generalized gradient approximation made simple, *Phys. Rev. Lett*. **77** (1996) 3865.